



Niels Bohr Institutet

FACULTY OF SCIENCE
UNIVERSITY OF COPENHAGEN

Bachelor's Thesis

Quantum Transport through Single and Double Quantum Dots

Iason Tsiamis

12 June, 2013

Supervisor: Dr Karsten Flensberg

Niels Bohr Institute
University of Copenhagen,
Universitetsparken 5,
Copenhagen 2100, Denmark

Contents

1	Introduction	4
1.1	Mathematical Tools	4
1.1.1	Second Quantization	4
2	2-D Electron Gas	5
3	Quantum Dots	7
3.1	Quantum Dots	7
3.1.1	General Features	7
3.1.2	Hamiltonian	8
3.1.3	Double Quantum Dots	9
3.2	Pauli Blockade	9
3.3	Coulomb Blockade	10
4	Master Equations	12
4.1	Sequential Tunnelling	12
4.2	Single Quantum Dot, with spin	13
4.3	Double Quantum Dot, without spin	14
4.4	Double Quantum Dot, with spin	17
5	Conclusions	21
6	Appendices	22
6.1	Double dot without spin (Matlab program)	22
6.2	Double dot with spin (Matlab program)	23

Abstract

We study the properties of single and double quantum dots. We focus on the transport of electrons between the dots and the source/drain, and between the first and second dot, in the case of the double dot. We analyse the systems of single dot, double dot without spin and double dot with spin. We find the possible states of each system and the transition rates between its states. We calculate the Master equations, which lead us to calculate the current, produced by the electron transfer, in each system. Finally, we create two programs, where one simulates the double dot system for electrons with and one for electrons without spin, and we compare qualitatively our results with the experimental data.

Chapter 1

Introduction

1.1 Mathematical Tools

1.1.1 Second Quantization

The main tool, used to describe many particle physical systems, is the second quantization. Main features of which are the creation and annihilation operators, which add or remove a particle (boson or fermion) to many-body wave functions, respectively. Below is presented the basic notation used in this thesis.

$c_{k\sigma}^\dagger$: creation fermion operator, creates an electron in state k with spin σ

$c_{k\sigma}$: annihilation fermion operator, annihilates an electron in state k with spin σ

And they act as following in the many-body wave-functions

$$c^\dagger |n_1 \dots n_i \dots\rangle = (-1)^{\sum^i} (1-i) C_+(n_{\nu_j}) |n_1 \dots n_{(i+1)} \dots\rangle$$

$$c |n_1 \dots n_i \dots\rangle = (-1)^{\sum^i} (1-i) C_-(n_{\nu_j}) |n_1 \dots n_{(i-1)} \dots\rangle$$

Anticommutation relations of fermion operators

$$\begin{aligned} \{c_{\nu_j}^\dagger, c_{\nu_k}^\dagger\} &= 0 \\ \{c_{\nu_j}, c_{\nu_k}\} &= 0 \\ \{c_{\nu_j}, c_{\nu_k}^\dagger\} &= \delta_{\nu_j \nu_k} \end{aligned}$$

Chapter 2

2-D Electron Gas

Electron gases of reduced dimensionality play a very important role in modern experimental physics. Especially two-dimensional electron gases in heterostructures are a fundamental part of semiconductor nanostructures.

The most recent type of them is the gallium arsenide/gallium-aluminium-arsenide (GaAs/GaAlAs) heterostructure.

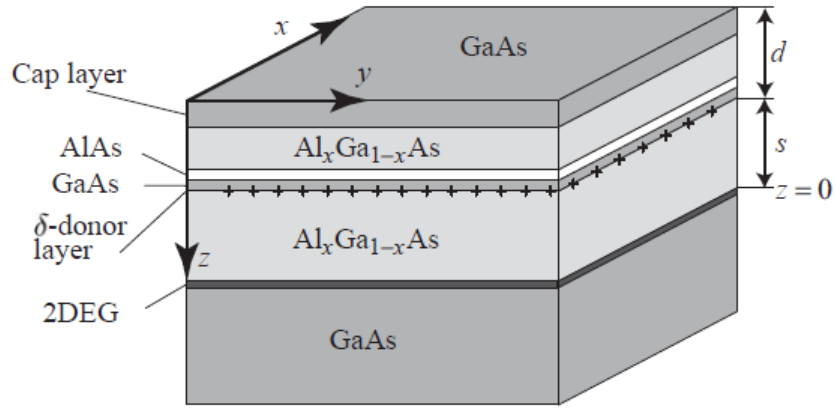


Figure 2.1: Layer sequence in a typical GaAs/AlGaAs heterostructure with remote doping.

Firstly we will examine the electrostatic properties of this structure, which is shown in the image above. We choose the z axis in the growth direction of the crystal, with its origin, $z=0$. For $z \gg 0$ the electric field in the sample is zero and the conduction band edge is flat. If we place a cylindrical close surface along z with one end face in the region $z \gg 0$ and the other in the region $-s < z < 0$, we can apply Gauss's law of electrodynamics and find the electric field in the spacer layer.

$$E = \frac{|e|n_s}{\epsilon\epsilon_0}$$

and the corresponding electrostatic potential

$$\Phi = \frac{|e|(n_s - N_d)}{\epsilon\epsilon_0}$$

If we extend the cylinder further in the negative z -direction, we include the δ -doping layer and we find the new value

$$E = \frac{|e|(n_s - N_d)}{\epsilon\epsilon_0}$$

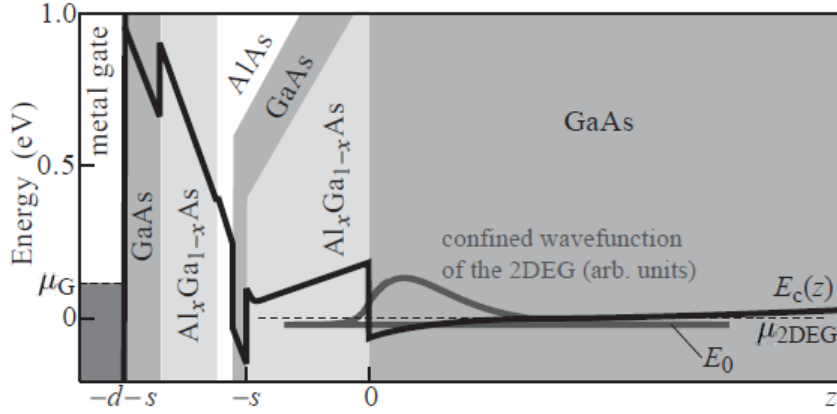


Figure 2.2: Effective potential for electrons in the conduction band in a typical GaAs/AlGaAs heterostructure with remote doping.

Owing the Fermi level pinning at the metal/GaAs interface the electro-chemical potential (Fermi level) at the surface is at the energy:

$$\mu_G = E_c(-s-d) - \Phi_b$$

where Φ_b is the built-in potential, which is half the band gap. Within the the electron gas the electrochemical potential which is given by the sum of the quantization energy and the Fermi energy:

$$\mu_{2DEG} = E_0(n_s) + E_F(n_s)$$

As a consequence, the relation between an applied gate voltage U_G between top gate and electron gas is

$$-eU_G = \mu_G - \mu_{2DEG} = -\frac{e^2 n_s}{\epsilon \epsilon_0} - \frac{e^2 (n_s - N_d)}{\epsilon \epsilon_0} d - \Phi_b - E_0(n_s) - E_F(n_s)$$

Chapter 3

Quantum Dots

3.1 Quantum Dots

3.1.1 General Features

A quantum dot is an artificially structured system that can be filled with electrons (or holes). It can be coupled with tunnel barriers to reservoirs, with which electrons can be exchanged.

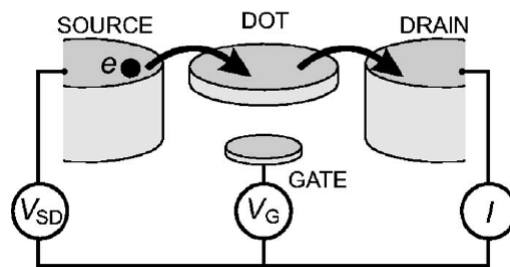


Figure 3.1: Schematic picture of a quantum dot in a lateral geometry.

As shown in figure 3.1, by applying voltage on these reservoirs, we can measure the electronic properties of the dot, examining the produced current. The dot is also coupled with a gate electrode, which is used to tune the electrostatic potential of the dot, with respect to the reservoirs.

The most popular quantum dots for experimental studies, are constructed from heterostructures of GaAs and AlGaAs grown by molecular-beam epitaxy. Whereas by doping the AlGaAs layer with Si, free electrons are introduced, forming a two-dimensional electron gas that can only move along the interface.

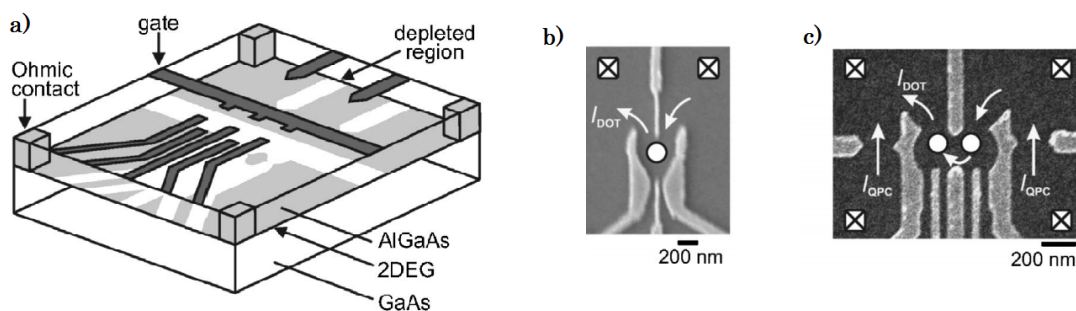


Figure 3.2: Lateral quantum dot device defined by metal surface electrodes. (a) Schematic view. (b),(c) Scanning electron micrographs of (b) a few-electron single-dot device and (c) a double dot device.

The electronic properties of quantum dots are dominated by two effects. Firstly, the Coulomb repulsion between electrons, leads to an energy cost in order to add an extra electron. Due to this fact tunnelling of electrons to or from the reservoirs can be suppressed at low temperatures, this phenomenon is called Coulomb blockade and we will focus on it later. The second effect is that the confinement in all three directions leads to quantum effects that influence the electron dynamics, resulting in a discrete energy spectrum.

The constant interaction model, is the model used to describe the electrostatic properties of quantum dots. It is based on two assumptions. First, the interactions among electrons in the dot and those in the environment are parametrized by a constant capacitance, which is the sum of the capacitances between the dot and the source, and the drain, and the gate, $C = C_S + C_D + C_G$.

The second assumption is that the single-particle energy-level spectrum is independent of these interactions and therefore of the number of electrons. Under these assumptions, the total energy $U(N)$ of a dot with N electrons in the ground state, with voltages V_S, V_D, V_G applied to the source, drain, gate respectively is given by the equation

$$U(N) = \frac{(-|e|(N - N_0) + C_S V_S + C_D V_D + C_G V_G)^2}{2C} + \sum_{n=1}^N E_n(B).$$

Where N_0 $|e|$ is the charge in the dot compensating the positive background charge originating from the donors in the heterostructure and B is the applied magnetic field. The terms $C_S V_S, C_D V_D, C_G V_G$, can be changed continuously and represent an effective induced charge that changes the electrostatic potential of the dot. The last term of the equation is a sum over the occupied single particle energy levels $E_n(B)$ which depend on the characteristics of the confinement potential. So, the electrochemical potential $\mu(N)$ of the dot is defined as

$$\mu(N) = U(N) - U(N - 1) = (N - N_0 - \frac{1}{2})E_C - \frac{E_C}{|e|}(C_S V_S + C_D V_D + C_G V_G) + E_N$$

3.1.2 Hamiltonian

The Hamiltonian describing the quantum dot system is

$$H = H_L + H_R + H_D + H_T$$

where H_L and H_R are the Hamiltonians for the left and the right leads, respectively (source and drain), H_D is the Hamiltonian describing the dot region and H_T is the tunnelling Hamiltonian, that couples these three subsystems.

$$H_T = H_{TL} + H_{TR}$$

with

$$H_{TL} = \sum_{\nu_D \nu_L} (t_{L, \nu_L, \nu_D} c_{\nu_L}^\dagger c_{\nu_D} + t_{L, \nu_L, \nu_D}^* c_{\nu_D}^\dagger c_{\nu_L})$$

$$H_{TR} = \sum_{\nu_D \nu_R} (t_{R, \nu_R, \nu_D} c_{\nu_R}^\dagger c_{\nu_D} + t_{R, \nu_R, \nu_D}^* c_{\nu_D}^\dagger c_{\nu_R})$$

where t is a tunnelling coefficient (e.g. t_{L, ν_L, ν_D} is the tunnelling coefficient from the state ν_L of left lead, to the state ν_D of the dot, whereas t_{L, ν_L, ν_D}^* is its complex conjugate, describing the exact opposite process) and the fermion operators $c_{\nu_D}^\dagger, c_{\nu_L}^\dagger, c_{\nu_R}^\dagger$ define the states in the uncoupled dot, the left lead and the right lead, respectively.

Finally, the dot Hamiltonian includes a single particle part and an interaction part $H_D = H_0 + H_{int}$, where the non interacting part is typically $H_0 = \sum_{\nu_D} \xi_{\nu_D} c_{\nu_D}^\dagger c_{\nu_D}$, while the interaction part is to be specified. In our system the dot Hamiltonian is

$$H_D = \sum_{\sigma=\uparrow\downarrow} \xi_{d\sigma} c_{d\sigma}^\dagger c_{d\sigma} + U n_{d\uparrow} n_{d\downarrow}.$$

3.1.3 Double Quantum Dots

We will now describe a system, where two quantum dots exist, dot 1 and dot 2, whose electrochemical potentials are controlled independently by the gate voltages $V_{G,1}$ and $V_{G,2}$, respectively.

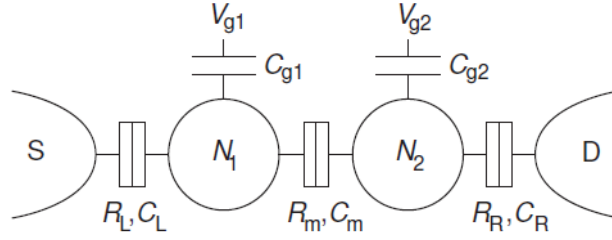


Figure 3.3: Network of resistors and capacitors representing two quantum dots coupled in series.

If the dots are completely uncoupled, their stability diagram, (N_1, N_2) as a function of $V_{G,1}$ and $V_{G,2}$, where N_1, N_2 are the number of electrons in dot 1 and 2, respectively, is shown on the figure 3.4(a). The lines indicate the values of the gate voltages, at which the number of the electrons in the ground state changes. We see that these lines are exactly horizontal and vertical on the the left diagram, since the electrochemical potential in each dot is independent of the charge in the other dot and each gate voltage only affects one of the dots.

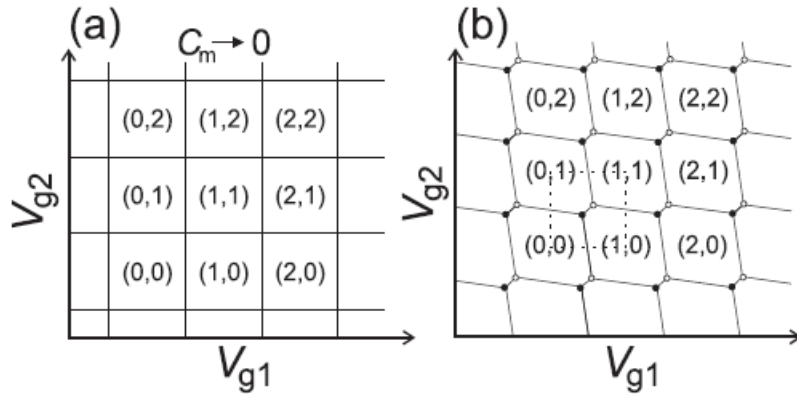


Figure 3.4: Schematic stability diagram of the double-dot system for (a) infinitesimal, (b) considerable inter-dot coupling.

If now the dots are capacitively coupled, addition of an electron on one dot, affects the electrostatic energy of the other dot. Also, the gate voltage of one dot, has also a direct capacitive coupling to the other dot. The resulting charge stability diagram, is shown right above, on figure 3.4(b). We see that each cross point is split into to so called "triple points". The triple points together form a hexagonal or "honeycomb" lattice. The fact is that at a triple point, three different charge states are energetically degenerate and the distance between the triple points is set by the capacitance between the two dots.

3.2 Pauli Blockade

Pauli blockade is a quantum effect, we encounter in the double quantum dots and is a result of the Pauli exclusion principle. At negative bias electrons are transferred through the device in the sequence $(0, 1) \rightarrow (0, 2) \rightarrow (1, 1) \rightarrow (0, 1)$. In this cycle the right dot always contains a single electron. Assume this electron is spin up. Then, in the transition $(0, 1) \rightarrow (0, 2)$ the right dot can only accept a spin-down electron from the leads due to Pauli exclusion, and a $S(0,2)$ state is formed. Similarly, only a spin-up electron can be added if the first electron is spin down. From $S(0,2)$, one electron can tunnel to the left dot and then out to the left lead. In contrast, when the bias voltage is positive charge transport proceeds in the sequence $(0, 1) \rightarrow (1, 1) \rightarrow (0, 2) \rightarrow (0, 1)$ and the left dot can be filled from

the Fermi sea with either a spin-up or a spin-down electron, regardless of the spin of the electron in the right dot. If the two electrons form a singlet state $S(1,1)$, the electron in the left dot can transfer to the right dot forming $S(0,2)$. However, if electrons form one of the triplet states $T(1,1)$, the electron in the left dot will not be able to tunnel to the right dot because $T(0,2)$ is too high in energy. The system will remain stuck in a $(1,1)$ charge state until the electron spin relaxes. Since the T_1 time can approach milliseconds, the current in this direction is negligible and the dot is said to be in spin blockade. Because it is the Pauli exclusion principle that forbids electrons to make a transition from a $T(1,1)$ state to $S(0,2)$, this blockade is also referred to as Pauli blockade. This effect leads to an asymmetry of the current as function of source-drain voltage, so it can be easily observed in an experiment.

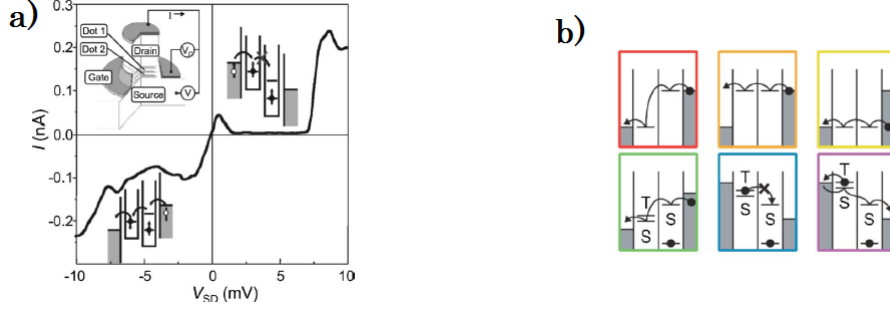


Figure 3.5: (a) Current (I) measured as a function of source-drain voltage (V) in a vertical double dot system. Nonzero current is measured over the entire range of negative voltage. For positive bias, current is blocked in the range $2 < V < 7$ mV. At bias voltages exceeding 7 mV, the $(0,2)$ triplet state becomes accessible and Pauli blockade is lifted. (b) Different ways of transport and Pauli blockade effect shown on the blue box.

3.3 Coulomb Blockade

The other effect that we encounter during the studying of quantum dots is the Coulomb blockade. On a qualitative level the Coulomb blockade effect can be described in a very intuitive and yet very general way.

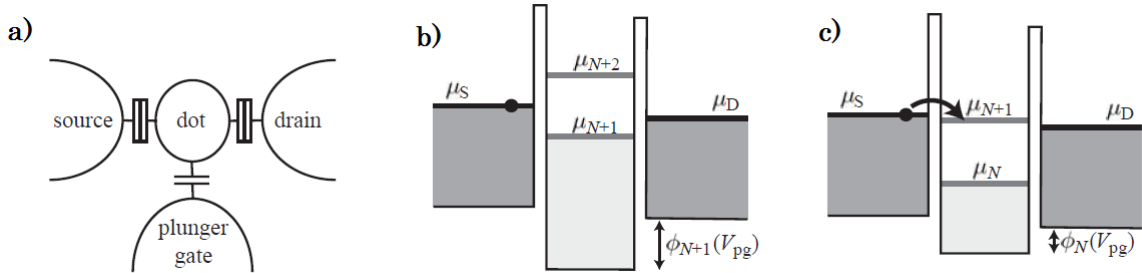


Figure 3.6: (a) Schematic representation of a quantum dot system with source and drain contacts and a plunger gate. (b) Energy level structure of the system in the Coulomb blockade. (c) Position of the energy levels that allows current to flow between source and drain if a very small bias voltage is applied.

Figures 3.6(b),(c) show the energetic situation in the three subsystems source, drain, and dot. At low temperature the electronic levels in the source (drain) contact are filled from the bottom of the conduction band up to the electrochemical potential μ_S (μ_D). In the quantum dot we can also define an electrochemical potential. It describes the energy necessary to add an electron to the dot, given that it is both initially and after the addition in its ground state. For example, if we consider a quantum dot with $N-1$ electrons initially, we define the electrochemical potential for adding the N th electron as

$$\mu_N(V_{pg}) = E_N(V_{pg}) - E_{N-1}(V_{pg})$$

The plunger gate voltage allows us to shift the levels $\mu_N(V_{pg})$ in energy. We find for the voltage dependence $\mu_N(V_{pg}) = \mu_N(V_{pg}^0) - |e|\alpha_{pg}\Delta V_{pg}$ which is independent of the electron number N . Using the plunger gate voltage we can tune the quantum dot electrochemical potentials into the position shown in the right side of the image above, where we have $\mu_S \simeq \mu_{N+1}(V_{pg})\mu_D$. In this case, the energy gain μ_S from removing an electron from the source contact is exactly equal to $\mu_{N+1}(V_{pg})$, the energy required to add an electron to the dot. Once the electron is in the dot, the energy gain $\mu_{N+1}(V_{pg})$ for removing it again is exactly equal to the energy μ_D required to add it to the drain contact. Therefore, elastic electron transport through the quantum dot is possible and the conductance measurement shows a large current at the respective plunger gate voltages. However, electrons can only tunnel one after another through the dot, because the energy difference $E_{N+2}^0(V_{pg}) - E_N^0(V_{pg})$ to add two electrons to the dot at the same time is significantly higher than the energy for a single electron. We therefore talk about sequential single-electron tunnelling. The situation of the current blockade is shown in figure 3.6(b), as well as in figures 3.7(a),(b),(c) for levels μ_{N+1}, μ_{N-1} . At this plunger gate voltage the dot is filled with $N + 1$ electrons. In order to fill the $(N + 2)$ th electron more energy is required than the energy gain from removing an electron from the source contact, i.e., $\mu_{N+2}(V_{pg}) > \mu_S, \mu_D$. The current flow is therefore blocked and we talk about Coulomb blockade. The separation ΔV_{pg} of neighbouring conductance resonances is found:

$$\Delta V_{pg} = \frac{\mu_{N+1}V_{pg}^0 - \mu_N(V_{pg}^0)}{|e|\alpha_{pg}}$$

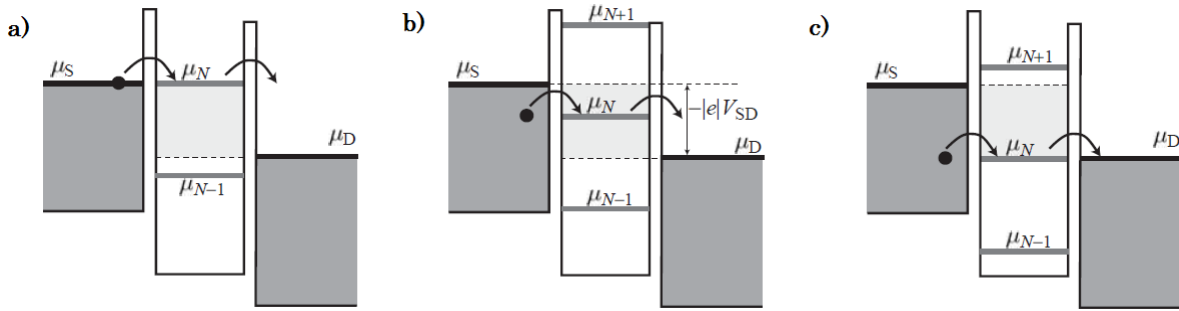


Figure 3.7: Schematic representation of a quantum dot system with finite applied bias for various plunger gate voltages. The energy region in light gray represents the so-called bias window. Arrows indicate electron transfer. (a) Current onset for $\mu_S = \mu_N(V_{pg})$. (b) Situation with $\mu_S > \mu_N(V_{pg}) > \mu_D$ (region of current flow). (c) Current onset at $\mu_D = \mu_N(V_{pg})$.

Chapter 4

Master Equations

4.1 Sequential Tunnelling

The sequential tunnelling regime, is equivalent to the weak tunnelling regime and it assumes that the time spent in the dot is much longer than the time between tunnelling events. So, in this regime, we can treat the mesoscopic system as an isolated system and describe it by a distribution function $P(\alpha)$, that gives the probability of finding the system in a particular state, α . In equilibrium $P(\alpha)$ is the Boltzmann distribution function

$$P(E_\alpha) = \frac{1}{Z} \exp(-\beta E_\alpha)$$

where E_α is the energy of state α , β is the inverse temperature and Z the normalization factor. However, when a voltage bias is applied across the system, we are no more in equilibrium conditions, so we analyse the transitions between the various α states, and according to the weak interaction model, we can use Fermi's golden rule with the tunnelling Hamiltonian as a perturbation. The transition from state α to state β due to tunnelling through the left junction is

$$\Gamma_{\beta\alpha}^L = 2\pi \sum_{f_\beta i_\alpha} |\langle f_\beta | H_{TL} | i_\alpha \rangle|^2 W_{i_\alpha} \delta(E_{f_\beta} - E_{i_\alpha}),$$

where the sum over initial states runs over all configurations of the internal degrees of freedom, i_α , that give state α , each weighted by a thermal distribution function W_{i_α} . Similarly, we sum over configurations of the final states that give the final state β . As for the $2\pi W_{i_\alpha} \delta(E_{f_\beta} - E_{i_\alpha})$ it changes into $\Gamma^L n_F(E_{\beta_{N+1}} - E_{\alpha_N} - \mu_L)$ while a transfer adds an electron and into $\Gamma^L (1 - n_F(E_{-\beta_{N-1}} + E_{\alpha_N} - \mu_L))$ while a transfer removes an electron, $\Gamma^L = 2\pi |t_L|^2 d_L$, while

$$n_F(x) = \frac{1}{\exp(x/T) + 1}.$$

Knowing the transition rates, we can set up the so called Master equations, for the dynamical behaviour of the distribution function $P(\alpha)$.

$$\frac{d}{dt} P(\alpha) = - \sum_{\beta} \Gamma_{\beta\alpha} P(\alpha) + \sum_{\beta} \Gamma_{\alpha\beta} P(\beta),$$

where the first term represents the tunnelling out of state α and the second the tunnelling into state α .

We are going to focus on the steady state, where $dP(\alpha)/dt=0$, and consequently

$$0 = - \sum_{\beta} \Gamma_{\beta\alpha} P(\alpha) + \sum_{\beta} \Gamma_{\alpha\beta} P(\beta)$$

Using the set of the master equations (for every state) in combination with the normalization condition $\sum_{\alpha} P(\alpha)=1$, the distribution function can be determined.

4.2 Single Quantum Dot, with spin

We have a single quantum dot, so we define the four possible states of the system, as $P(0), P(1u), P(1d), P(2)$, where the first state is empty, the second is singly occupied with one electron spin up, the third singly occupied with spin down and the fourth doubly occupied. About the energies of each state $E_0=0$, E_{1u} and E_{1d} depend only on the gate voltage (V_G) and $E_2 = E_{1u} + E_{1d} + U$, where U is the interaction energy, between the electrons in the dot.

The transition rates are:

$$\begin{aligned}
\Gamma_{1u0} &= \Gamma^L |\langle 1u | c_{1u}^\dagger | 0 \rangle|^2 n_F(E_{1u} - E_0 - \mu_L) + \Gamma^R |\langle 1u | c_{1u}^\dagger | 0 \rangle|^2 n_F(E_{1u} - E_0 - \mu_R) \\
\Gamma_{1d0} &= \Gamma^L |\langle 1d | c_{1d}^\dagger | 0 \rangle|^2 n_F(E_{1d} - E_0 - \mu_L) + \Gamma^R |\langle 1d | c_{1d}^\dagger | 0 \rangle|^2 n_F(E_{1d} - E_0 - \mu_R) \\
\Gamma_{01d} &= \Gamma^L |\langle 0 | c_{1d} | 1d \rangle|^2 (1 - n_F(E_{1d} - E_0 - \mu_L)) + \Gamma^R |\langle 1d | c_{1d} | 0 \rangle|^2 (1 - n_F(E_{1d} - E_0 - \mu_R)) \\
\Gamma_{01u} &= \Gamma^L |\langle 0 | c_{1u} | 1u \rangle|^2 (1 - n_F(E_{1u} - E_0 - \mu_L)) + \Gamma^R |\langle 1u | c_{1u} | 0 \rangle|^2 (1 - n_F(E_{1u} - E_0 - \mu_R)) \\
\Gamma_{21u} &= \Gamma^L |\langle 2 | c_{1d}^\dagger | 1u \rangle|^2 n_F(E_2 - E_{1u} - \mu_L) + \Gamma^R |\langle 2 | c_{1d}^\dagger | 1u \rangle|^2 n_F(E_2 - E_{1u} - \mu_R) \\
\Gamma_{21d} &= \Gamma^L |\langle 2 | c_{1u}^\dagger | 1d \rangle|^2 n_F(E_2 - E_{1d} - \mu_L) + \Gamma^R |\langle 2 | c_{1u}^\dagger | 1d \rangle|^2 n_F(E_2 - E_{1d} - \mu_R) \\
\Gamma_{1u2} &= \Gamma^L |\langle 1u | c_{1d} | 2 \rangle|^2 (1 - n_F(E_2 - E_{1u} - \mu_L)) + \Gamma^R |\langle 1u | c_{1d} | 2 \rangle|^2 (1 - n_F(E_2 - E_{1u} - \mu_R)) \\
\Gamma_{1d2} &= \Gamma^L |\langle 1d | c_{1u} | 2 \rangle|^2 (1 - n_F(E_2 - E_{1d} - \mu_L)) + \Gamma^R |\langle 1d | c_{1u} | 2 \rangle|^2 (1 - n_F(E_2 - E_{1d} - \mu_R))
\end{aligned}$$

Once we calculate the inner products, the rest are constants referred to the natural properties of the system, found in the eight transition equations above, we form the four master equations:

$$\begin{aligned}
\Gamma_{01u}P(1u) + \Gamma_{01d}P(1d) - (\Gamma_{01u} + \Gamma_{01d})P(0) &= 0 \\
\Gamma_{1u0}P(0) + \Gamma_{1u2}P(2) - (\Gamma_{01u} + \Gamma_{21u})P(1u) &= 0 \\
\Gamma_{1d0}P(0) + \Gamma_{1d2}P(2) - (\Gamma_{01d} + \Gamma_{21d})P(1d) &= 0 \\
\Gamma_{21u}P(1u) + \Gamma_{21d}P(1d) - (\Gamma_{1u2} + \Gamma_{1d2})P(2) &= 0.
\end{aligned}$$

Because we have four unknown distribution functions $P(0), P(1u), P(1d), P(2)$ and three out of these four equations are linearly independent, we also use the normalization equation, replacing one of the previous four with it, in order to have a 4-linearly independent equations system.

$$P(0) + P(1u) + P(1d) + P(2) = 1$$

In order to solve this 4-equation system we define the P row vector, $P = \begin{pmatrix} P(0) \\ P(1u) \\ P(1d) \\ P(2) \end{pmatrix}$, so the system can be now written as a matrix product of a 4x4 matrix A and vector P equals a constant.

$$\text{So } A = \begin{pmatrix} -(\Gamma_{1u0} + \Gamma_{1d0}) & \Gamma_{01u} & \Gamma_{01d} & 0 \\ \Gamma_{1u0} & -(\Gamma_{01u} + \Gamma_{21u}) & 0 & \Gamma_{1u2} \\ \Gamma_{1d0} & 0 & -(\Gamma_{01d} + \Gamma_{21d}) & \Gamma_{1d2} \\ 1 & 1 & 1 & 1 \end{pmatrix} \text{ and } C = \begin{pmatrix} 0 \\ 0 \\ 0 \\ 1 \end{pmatrix} \text{ the constant.}$$

So now we can write the 4-equations' system as $AP = C$, and in order to find P which is the vector of the distribution functions, we just have to calculate $P = A^{-1}C$.

Having calculated the values of the distribution functions, we can now measure the value of the current due to the transport of electrons between source and drain, by the sum of the transition rates that add an electron to the dot minus the sum of those that remove one from the dot, towards one direction (in this case "left") and multiplied by the electron's charge. A value that can be compared with experimental results and show us, to what extent, our model corresponds to reality.

$$I = (-e) \sum_N (\Gamma_{N+1,N}^L - \Gamma_{N-1,N}^L) P(N)$$

$$I = (-e)(\Gamma_{21d}^L P(1d) + \Gamma_{21u}^L P(1u) - \Gamma_{1u2}^L P(2) - \Gamma_{1d2}^L P(2))$$

4.3 Double Quantum Dot, without spin

In this section we will describe a double dot, which is a structure of two dots in a row, the first coupled with the left lead and with the second dot, while the second dot is coupled with the right lead, apart from the first dot. The problem we encounter in this system is that the tunnelling between dot 1 and dot 2, cannot be described with the transitions rates explained above, because there is no electron sea (as it happens with the rest transitions e.g. in source-dot 1 transition, the source is an electron sea), and the Fermi's golden rule cannot be applied. In order to overcome this problem, we use the Hamiltonian of the system in order to find the two eigenstates, which will be uncoupled between them, but coupled with the left and right lead, making it possible to use Fermi's golden rule and furthermore the transition rates equations, used above. The Hamiltonian of the system is $H_{1e} = \begin{pmatrix} |\langle \Phi_1 | H | \Phi_1 \rangle| & |\langle \Phi_1 | H | \Phi_2 \rangle| \\ |\langle \Phi_2 | H | \Phi_1 \rangle| & |\langle \Phi_2 | H | \Phi_2 \rangle| \end{pmatrix} = \begin{pmatrix} \varepsilon_1 & -t \\ -t & \varepsilon_2 \end{pmatrix}$, where t is the coupling of the wave functions of the two dots and Φ_1, Φ_2 are the wave functions of the dot 1 and 2, respectively. Finding the eigenvalues and eigenvectors of this Hamiltonian, we find the energies and eigenstates of the system. The energies of the two states are

$$E_A = \frac{\varepsilon_1 + \varepsilon_2 + \sqrt{(\varepsilon_1 - \varepsilon_2)^2 + 4t^2}}{2}$$

$$E_B = \frac{\varepsilon_1 + \varepsilon_2 - \sqrt{(\varepsilon_1 - \varepsilon_2)^2 + 4t^2}}{2}$$

and the two states are found as $|A\rangle = u_1|1\rangle + v_1|2\rangle$ and $|B\rangle = -v_1|1\rangle + u_1|2\rangle$, where u_1, v_1 the normalized elements of the eigenvectors, and $|1\rangle$ and $|2\rangle$ are the states describing dot 1 and dot 2. So now, the system states can be rewritten, using second quantization, in the language of fermion operators as

$$\begin{aligned} |0\rangle & \\ |A\rangle &= c_A^\dagger |0\rangle \\ |B\rangle &= c_B^\dagger |0\rangle \\ |2\rangle &= c_A^\dagger c_B^\dagger |0\rangle \end{aligned}$$

where $c_A^\dagger = uc_1^\dagger + vc_2^\dagger$ and $c_B^\dagger = -vc_1^\dagger + uc_2^\dagger$.

Using the new state operators, we calculate the transitions rates, the results are listed below.

$$\begin{aligned} \Gamma_{A0} &= \Gamma^L u^2 n_F(E_A - E_0 - \mu_L) + \Gamma^R v^2 n_F(E_A - E_0 - \mu_R) \\ \Gamma_{B0} &= \Gamma^L v^2 n_F(E_B - E_0 - \mu_L) + \Gamma^R u^2 n_F(E_B - E_0 - \mu_R) \\ \Gamma_{2A} &= \Gamma^L ((u^2 - v^2)v)^2 n_F(E_2 - E_A - \mu_L) + \Gamma^R ((u^2 - v^2)u)^2 n_F(E_2 - E_A - \mu_R) \\ \Gamma_{2B} &= \Gamma^L ((u^2 - v^2)u)^2 n_F(E_2 - E_B - \mu_L) + \Gamma^R ((v^2 - u^2)v)^2 n_F(E_2 - E_B - \mu_R) \\ \Gamma_{0A} &= \Gamma^L u^2 (1 - n_F(E_A - E_0 - \mu_L)) + \Gamma^R v^2 (1 - n_F(E_A - E_0 - \mu_R)) \\ \Gamma_{0B} &= \Gamma^L v^2 (1 - n_F(E_B - E_0 - \mu_L)) + \Gamma^R u^2 (1 - n_F(E_B - E_0 - \mu_R)) \\ \Gamma_{A2} &= \Gamma^L ((u^2 - v^2)v)^2 (1 - n_F(E_2 - E_A - \mu_L)) + \Gamma^R ((u^2 - v^2)u)^2 (1 - n_F(E_2 - E_A - \mu_R)) \\ \Gamma_{B2} &= \Gamma^L ((u^2 - v^2)u)^2 (1 - n_F(E_2 - E_B - \mu_L)) + \Gamma^R ((v^2 - u^2)v)^2 (1 - n_F(E_2 - E_B - \mu_R)) \end{aligned}$$

where, $E_2 = E_A + E_B + U_{12}$, where U_{12} is the energy of the interaction between the electron in dot 1 and the one in dot 2 and $E_0 = 0$.

Using the values of the transition rates we end up with the Master equations:

$$\begin{aligned} & P(0)(\Gamma^L u^2 n_F(E_A - E_0 - \mu_L) + \Gamma^R v^2 n_F(E_A - E_0 - \mu_R)) \\ & + \Gamma^L v^2 n_F(E_B - E_0 - \mu_L) + \Gamma^R u^2 n_F(E_B - E_0 - \mu_R)) \\ & - P(A)(\Gamma^L u^2 (1 - n_F(E_A - E_0 - \mu_L)) + \Gamma^R v^2 (1 - n_F(E_A - E_0 - \mu_R))) \\ & - P(B)(\Gamma^L v^2 (1 - n_F(E_B - E_0 - \mu_L)) + \Gamma^R u^2 (1 - n_F(E_B - E_0 - \mu_R))) = 0 \end{aligned}$$

$$\begin{aligned} & P(A)(\Gamma^L ((u^2 - v^2)v)^2 n_F(E_2 - E_A - \mu_L) + \Gamma^R ((u^2 - v^2)u)^2 n_F(E_2 - E_A - \mu_R)) \\ & + P(B)(\Gamma^L ((u^2 - v^2)u)^2 n_F(E_2 - E_B - \mu_L) + \Gamma^R ((v^2 - u^2)v)^2 n_F(E_2 - E_B - \mu_R)) \\ & - P(2)(\Gamma^L ((u^2 - v^2)v)^2 (1 - n_F(E_2 - E_A - \mu_L)) + \Gamma^R ((u^2 - v^2)u)^2 (1 - n_F(E_2 - E_A - \mu_R))) \\ & + \Gamma^L ((u^2 - v^2)u)^2 (1 - n_F(E_2 - E_B - \mu_L)) + \Gamma^R ((u^2 - v^2)v)^2 (1 - n_F(E_2 - E_B - \mu_R))) = 0 \end{aligned}$$

$$\begin{aligned} & P(A)(\Gamma^L ((u^2 - v^2)v)^2 n_F(E_2 - E_A - \mu_L) + \Gamma^R ((u^2 - v^2)u)^2 n_F(E_2 - E_A - \mu_R)) \\ & - (\Gamma^L u^2 (1 - n_F(E_A - E_0 - \mu_L)) + \Gamma^R v^2 (1 - n_F(E_A - E_0 - \mu_R))) \\ & + P(0)(\Gamma^L u^2 n_F(E_A - E_0 - \mu_L) + \Gamma^R v^2 n_F(E_A - E_0 - \mu_R)) \\ & - P(2)(\Gamma^L ((u^2 - v^2)v)^2 (1 - n_F(E_2 - E_A - \mu_L)) + \Gamma^R ((u^2 - v^2)u)^2 (1 - n_F(E_2 - E_A - \mu_R))) = 0 \end{aligned}$$

$$\begin{aligned} & P(B)(\Gamma^L ((u^2 - v^2)u)^2 n_F(E_2 - E_B - \mu_L) + \Gamma^L ((u^2 - v^2)u)^2 n_F(E_2 - E_B - \mu_L)) \\ & - \Gamma^L v^2 (1 - n_F(E_B - E_0 - \mu_L)) + \Gamma^R u^2 (1 - n_F(E_B - E_0 - \mu_R)) \\ & + P(0)(\Gamma^L v^2 n_F(E_B - E_0 - \mu_L) + \Gamma^R u^2 n_F(E_B - E_0 - \mu_R)) \\ & - P(2)(\Gamma^L ((u^2 - v^2)u)^2 (1 - n_F(E_2 - E_B - \mu_L)) + \Gamma^R ((u^2 - v^2)v)^2 (1 - n_F(E_2 - E_B - \mu_R))) = 0 \end{aligned}$$

Using the exact same technique as for the single dot, exchanging one of the four Master equations with the normalization principle, we end up with the distribution function vector P . By knowing all these we can finally calculate the current produced during the electron transport.

$$\begin{aligned} I &= P(0)(\Gamma^L u^2 n_F(E_A - E_0 - \mu_L) + \Gamma^L v^2 n_F(E_B - E_0 - \mu_L)) \\ & + P(A)(-\Gamma^L u^2 (1 - n_F(E_A - E_0 - \mu_L)) + \Gamma^L ((u^2 - v^2)v)^2 n_F(E_2 - E_A - \mu_L)) \\ & + P(B)(\Gamma^L ((u^2 - v^2)u)^2 n_F(E_2 - E_B - \mu_L) - \Gamma^L v^2 (1 - n_F(E_B - E_0 - \mu_L))) \\ & - P(2)(\Gamma^L ((u^2 - v^2)v)^2 (1 - n_F(E_2 - E_A - \mu_L)) + \Gamma^L ((u^2 - v^2)u)^2 (1 - n_F(E_2 - E_B - \mu_L))) \end{aligned}$$

We use all the equations written above, in order to make a simulation program. Because the computer works with numbers, without units, we use the following transformations of the parameters:

$$\begin{aligned} \tilde{I} &= \frac{I}{E(\Gamma^L + \Gamma^R)} \\ \tilde{\Gamma}^L &= \frac{\Gamma^L}{E(\Gamma^L + \Gamma^R)} \\ \tilde{\varepsilon}_1 &= \frac{\varepsilon_1}{t} \\ \tilde{\varepsilon}_2 &= \frac{\varepsilon_2}{t} \\ \mu_L - \mu_R &= eV \end{aligned}$$

The first result we get is the plot of $I=f(V)$, and is shown on figure 4.1(a),(b), where V is the voltage applied between the source and the drain. As we can observe, the graph is symmetrical and there is no current before a value $V_1 = |2, 5|$, where the energy level of the source becomes equal to the energy of the lower energy state. After that we have a constant current until we reach the second important value $V_2 = |6, 5|$ where the current instantly takes a higher value and stays there for the rest of the values of V . This second level is the point at which the energy level of the source becomes equal to the higher state, so now, there are two ways, for the electrons from the source to reach the drain (through eigenstate $|A\rangle$ and $|B\rangle$), for this reason the current is higher.

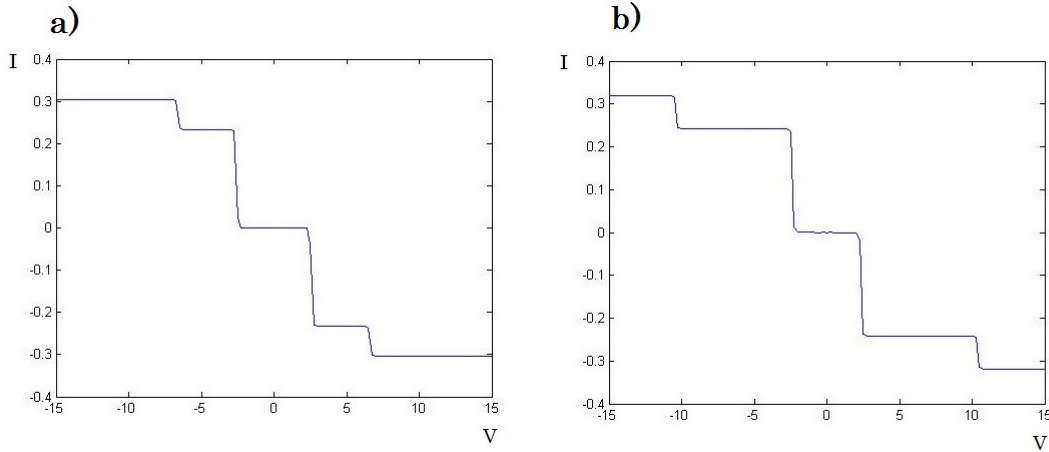


Figure 4.1: The resulting current as a function of drain-source voltage ($I=f(V)$) for (a) energy of dot 1 $\epsilon_1 = 2$ and energy of dot 2 $\epsilon_2 = 1$, (b) doubled energy of dot 1 $\epsilon_1 = 4$ and the same energy of dot 2 $\epsilon_2 = 1$.

Another characteristic that we observed is that when we doubled the ϵ_2 energy of the second dot, the energy of the difference between V_1 and V_2 is doubled, as we can see on figure 4.1(b).

The second result that we get is the $I = f(\epsilon_1, \epsilon_2)$, which is helpful in order to understand the qualitative behaviour of the charge capacity diagram which is the graph $dI/d\epsilon_1 = f(\epsilon_1, \epsilon_2)$. Unfortunately we could not include this graph, because ϵ_1, ϵ_2 , also affected the Hamiltonian, making difficult for us to find the derivative.

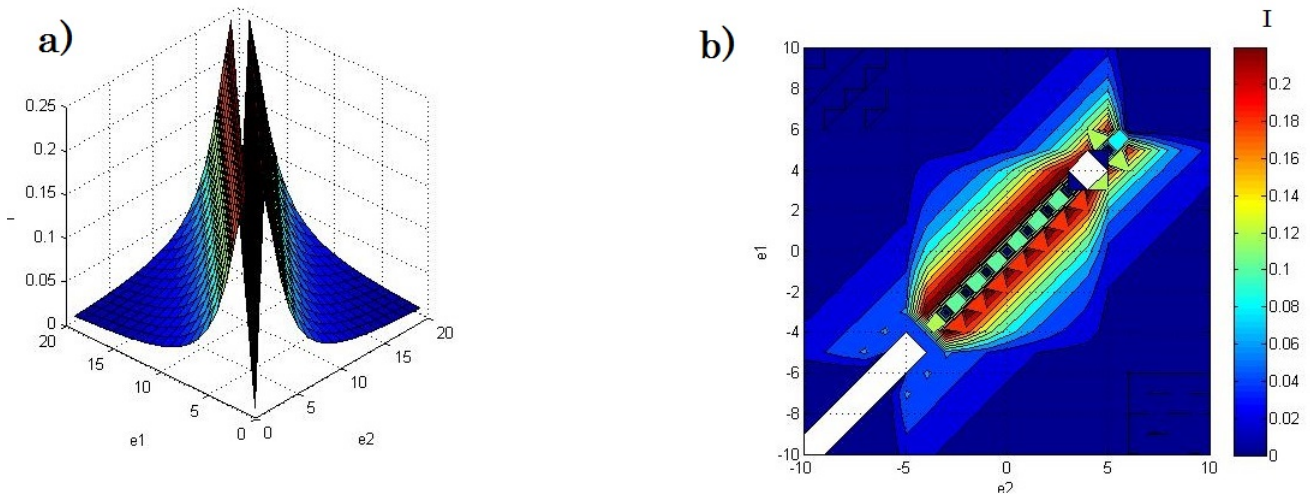


Figure 4.2: 3D plot of the resulting current as a function of the energy of dot 1 (ϵ_1) and the energy of dot 2 (ϵ_2), (a) each of the three elements is represented on an axis, (b) the dot energies energies are represented on axes and the resulting current is displayed on colour scale.

In figures 4.2(a),(b), we can get an idea of what the capacity diagram would look like, by watching the first image and try to imagine the derivative of ϵ_1 , we can clearly see two main and powerful lines of current, which refer to the two dots, by looking at the second dot, we can see that there is an angle of the ϵ_1 axis and the main current lines, if we imagine the derivative of the current lines, would clearly have a curve. The other factor is that in between the two current lines you can see that while there is almost no current in the center of the graph there is a small quantity of it, that is the current of the interdot transport and we can imagine that with the curvature of the derivative of ϵ_1 , it could have been even closer to the experimental results shown in figure 4.3. What we would have seen in a charge capacity diagram, would have been like the part of figure 4.3, that is limited in the white box.

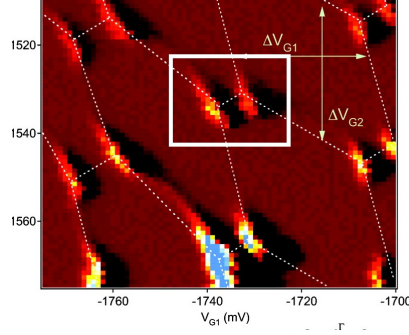


Figure 4.3: Colour scale displays dI/dV_{G_1} calculated from dc current (IDC) at $V_{SD} = 500 \mu V$. White lines are guides to the eye showing the honeycomb pattern of peaks in conductance. (Experimental charge stability diagrams for the series double quantum dot as a function of two gate voltages, each shifting the energy levels of a single dot)

4.4 Double Quantum Dot, with spin

We are now going to examine the last system in this thesis, the double quantum dot, taking the spin of the electrons under consideration. The Hamiltonian that describes this system is

$$H = \sum_{\sigma} \epsilon_{1\sigma} c_{1\sigma}^{\dagger} c_{1\sigma} + \epsilon_{2\sigma} c_{2\sigma}^{\dagger} c_{2\sigma} + t(c_{1\sigma}^{\dagger} c_{2\sigma} + c_{2\sigma}^{\dagger} c_{1\sigma}) + U_{12} n_1 n_2 + U_2 n_{2u} n_{2d}$$

Where $U_{12} n_1 n_2$ is the energy of the interaction of an electron in dot 1 with one in dot 2 and $U_2 n_{2u} n_{2d}$ is the energy of the interaction between two electrons in the second dot.

We calculate the matrix elements of the Hamiltonian in the same way as we did for the without spin case. Whereas, now we have five possible states for the case of 2 electrons in the system:

$$\begin{aligned} |T_0\rangle &= \frac{1}{\sqrt{2}}(c_{1\uparrow}^{\dagger} c_{2\downarrow}^{\dagger} + c_{1\downarrow}^{\dagger} c_{2\uparrow}^{\dagger})|0\rangle \\ |T_+\rangle &= c_{1\uparrow}^{\dagger} c_{2\uparrow}^{\dagger}|0\rangle \\ |T_-\rangle &= c_{1\downarrow}^{\dagger} c_{2\downarrow}^{\dagger}|0\rangle \\ |S\rangle &= \frac{1}{\sqrt{2}}(c_{1\uparrow}^{\dagger} c_{2\downarrow}^{\dagger} - c_{1\downarrow}^{\dagger} c_{2\uparrow}^{\dagger})|0\rangle \\ |02\rangle &= c_{2\uparrow}^{\dagger} c_{2\downarrow}^{\dagger}|0\rangle \end{aligned}$$

So the matrix Hamiltonian for 2 electrons is the on below:

$$H_{2e} = \begin{pmatrix} \frac{\varepsilon_{1\uparrow} + \varepsilon_{1\downarrow} + \varepsilon_{2\uparrow} + \varepsilon_{2\downarrow}}{2} + U_{12}n_1n_2 & 0 & 0 & 0 & 0 \\ 0 & \varepsilon_{1\uparrow} + \varepsilon_{2\uparrow} + U_{12}n_1n_2 & 0 & 0 & 0 \\ 0 & 0 & \varepsilon_{1\downarrow} + \varepsilon_{2\downarrow} + U_{12}n_1n_2 & 0 & 0 \\ 0 & 0 & 0 & \frac{\varepsilon_{1\uparrow} + \varepsilon_{1\downarrow} + \varepsilon_{2\uparrow} + \varepsilon_{2\downarrow}}{2} + U_{12}n_1n_2 & \frac{t}{\sqrt{2}} \\ 0 & 0 & 0 & \frac{t}{\sqrt{2}} & \varepsilon_{2\uparrow} + \varepsilon_{2\downarrow} + U_{12}n_1n_2 + U_{2n_2u}n_{2d} \end{pmatrix}$$

where $\varepsilon_{1\uparrow}, \varepsilon_{2\downarrow}$ are the energies of an electron in the first dot with spin up and an electron in the second dot with spin down, respectively. We can observe that tunnelling can be achieved only between the two singlet states, a result that was expected. We have two more Hamiltonians in this problem one for three electrons and one for one electron. Although, there is no coupling between their states, so we will just mention the states.

$$\begin{aligned} |2d\rangle &= c_{2\downarrow}^\dagger |0\rangle \\ |2u\rangle &= c_{2\uparrow}^\dagger |0\rangle \\ |21d\rangle &= c_{1\downarrow}^\dagger c_{2\uparrow}^\dagger c_{2\downarrow}^\dagger |0\rangle \\ |21u\rangle &= c_{1\uparrow}^\dagger c_{2\uparrow}^\dagger c_{2\downarrow}^\dagger |0\rangle \end{aligned}$$

where $|2d\rangle, |2u\rangle$ are the states in which the second dot is occupied by one electron of spin down and spin up, respectively and $|21d\rangle, |21u\rangle$ are the states in which the second dot is occupied by two electrons (spin up and down, due to Pauli exclusion principle) and the first dot is occupied by one electron of spin down and spin up, respectively.

Following the same steps as in the previous systems, we calculate the transfer rates, which are listed bellow, which we use to the Master equations in order to find the distribution functions and calculate the current.

$$\begin{aligned} \Gamma_{T_0 2u} &= \Gamma^L \frac{1}{2} n_F(E_{T_0} - E_{2u} - \mu_L) \\ \Gamma_{T_p 2u} &= \Gamma^L n_F(E_{T_p} - E_{2u} - \mu_L) \\ \Gamma_{T_m 2u} &= 0 \\ \Gamma_{S_1 2u} &= \Gamma^L \frac{u^2}{2} n_F(E_{S_1} - E_{2u} - \mu_L) + \Gamma^R v^2 n_F(E_{S_1} - E_{2u} - \mu_R) \\ \Gamma_{S_2 2u} &= \Gamma^L \frac{v^2}{2} n_F(E_{S_2} - E_{2u} - \mu_L) + \Gamma^R u^2 n_F(E_{S_2} - E_{2u} - \mu_R) \\ \Gamma_{T_0 2d} &= \Gamma^L \frac{1}{2} n_F(E_{T_0} - E_{2d} - \mu_L) \\ \Gamma_{T_p 2d} &= 0 \\ \Gamma_{T_m 2d} &= \Gamma^L n_F(E_{T_m} - E_{2d} - \mu_L) \\ \Gamma_{S_1 2d} &= \Gamma^L \frac{u^2}{2} n_F(E_{S_1} - E_{2d} - \mu_L) + \Gamma^R v^2 n_F(E_{S_1} - E_{2d} - \mu_R) \\ \Gamma_{S_2 2d} &= \Gamma^L \frac{v^2}{2} n_F(E_{S_2} - E_{2d} - \mu_L) + \Gamma^R u^2 n_F(E_{S_2} - E_{2d} - \mu_R) \end{aligned}$$

$$\begin{aligned}
\Gamma_{T_0 12u} &= \Gamma^R \frac{1}{2} (1 - n_F(E_{12u} - E_{T_0} - \mu_R)) \\
\Gamma_{T_p 12u} &= \Gamma^R (1 - n_F(E_{12u} - E_{T_p} - \mu_R)) \\
\Gamma_{T_m 12u} &= 0 \\
\Gamma_{S_1 12u} &= \Gamma^L v^2 (1 - n_F(E_{12u} - E_{S_1} - \mu_L)) + \Gamma^R \frac{u^2}{2} (1 - n_F(E_{12u} - E_{S_1} - \mu_R)) \\
\Gamma_{S_2 12u} &= \Gamma^L u^2 (1 - n_F(E_{12u} - E_{S_2} - \mu_L)) + \Gamma^R \frac{v^2}{2} (1 - n_F(E_{12u} - E_{S_2} - \mu_R)) \\
\Gamma_{T_0 12d} &= \Gamma^R \frac{1}{2} (1 - n_F(E_{12d} - E_{T_0} - \mu_R)) \\
\Gamma_{T_p 12d} &= 0 \\
\Gamma_{T_m 12d} &= \Gamma^R (1 - n_F(E_{12d} - E_{T_m} - \mu_R)) \\
\Gamma_{S_1 12d} &= \Gamma^L v^2 (1 - n_F(E_{S_1} - E_{12d} - \mu_L)) + \Gamma^R \frac{u^2}{2} (1 - n_F(E_{S_1} - E_{12d} - \mu_R)) \\
\Gamma_{S_2 12d} &= \Gamma^L u^2 (1 - n_F(E_{12d} - E_{S_2} - \mu_L)) + \Gamma^R \frac{v^2}{2} (1 - n_F(E_{12d} - E_{S_2} - \mu_R)) \\
\Gamma_{2uT_0} &= \Gamma^L \frac{1}{2} (n_F(E_{T_0} - E_{2u} - \mu_L)) \\
\Gamma_{2uT_p} &= \Gamma^L (n_F(E_{T_p} - E_{2u} - \mu_L)) \\
\Gamma_{2uT_m} &= 0 \\
\Gamma_{2uS_1} &= \Gamma^L \frac{u^2}{2} (n_F(E_{S_1} - E_{2u} - \mu_L)) + \Gamma^R v^2 (n_F(E_{S_1} - E_{2u} - \mu_R)) \\
\Gamma_{2uS_2} &= \Gamma^L \frac{v^2}{2} (n_F(E_{S_2} - E_{2u} - \mu_L)) + \Gamma^R u^2 (n_F(E_{S_2} - E_{2u} - \mu_R)) \\
\Gamma_{2dT_0} &= \Gamma^L \frac{1}{2} (n_F(E_{T_0} - E_{2d} - \mu_L)) \\
\Gamma_{2dT_p} &= 0 \\
\Gamma_{2dT_m} &= \Gamma^L (n_F(E_{T_p} - E_{2d} - \mu_L)) \\
\Gamma_{2dS_1} &= \Gamma^L \frac{u^2}{2} (n_F(E_{S_1} - E_{2d} - \mu_L)) + \Gamma^R v^2 (n_F(E_{S_1} - E_{2d} - \mu_R)) \\
\Gamma_{2dS_2} &= \Gamma^L \frac{v^2}{2} (n_F(E_{S_2} - E_{2d} - \mu_L)) + \Gamma^R u^2 (n_F(E_{S_2} - E_{2d} - \mu_R)) \\
\Gamma_{12uT_0} &= \Gamma^R \frac{1}{2} (1 - n_F(E_{12u} - E_{T_0} - \mu_R)) \\
\Gamma_{12uT_p} &= \Gamma^R (1 - n_F(E_{12u} - E_{T_p} - \mu_R)) \\
\Gamma_{12uT_m} &= 0 \\
\Gamma_{12uS_1} &= \Gamma^L v^2 (1 - n_F(E_{12u} - E_{S_1} - \mu_L)) + \Gamma^R \frac{u^2}{2} (1 - n_F(E_{12u} - E_{S_1} - \mu_R)) \\
\Gamma_{12uS_2} &= \Gamma^L u^2 (1 - n_F(E_{12u} - E_{S_2} - \mu_L)) + \Gamma^R \frac{v^2}{2} (1 - n_F(E_{12u} - E_{S_2} - \mu_R)) \\
\Gamma_{12dT_0} &= \Gamma^R \frac{1}{2} (1 - n_F(E_{12d} - E_{T_0} - \mu_R)) \\
\Gamma_{12dT_p} &= 0 \\
\Gamma_{12dT_m} &= \Gamma^R (1 - n_F(E_{12d} - E_{T_m} - \mu_R)) \\
\Gamma_{12dS_1} &= \Gamma^L v^2 (1 - n_F(E_{12d} - E_{S_1} - \mu_L)) + \Gamma^R \frac{u^2}{2} (1 - n_F(E_{12d} - E_{S_1} - \mu_R)) \\
\Gamma_{12dS_2} &= \Gamma^L u^2 (1 - n_F(E_{12d} - E_{S_2} - \mu_L)) + \Gamma^R \frac{v^2}{2} (1 - n_F(E_{12d} - E_{S_2} - \mu_R))
\end{aligned}$$

Using the same process as before, but a bit more complicated, we end up with the following results. First, we see clearly on the $I=f(V)$ plot, the asymmetry, caused by the Pauli blockade (image shown below on the left). Furthermore, we have only one possible current value, which can be observed and that is, because as explained in the section 3.2, there is only one possible way for an electron to travel from the source to the drain (in the energy values that our system is limited in). Below on the right, we can see some experimental data of Pauli blockade. We care only about the first pick on the right, because only this is within the energetic limit of our model.

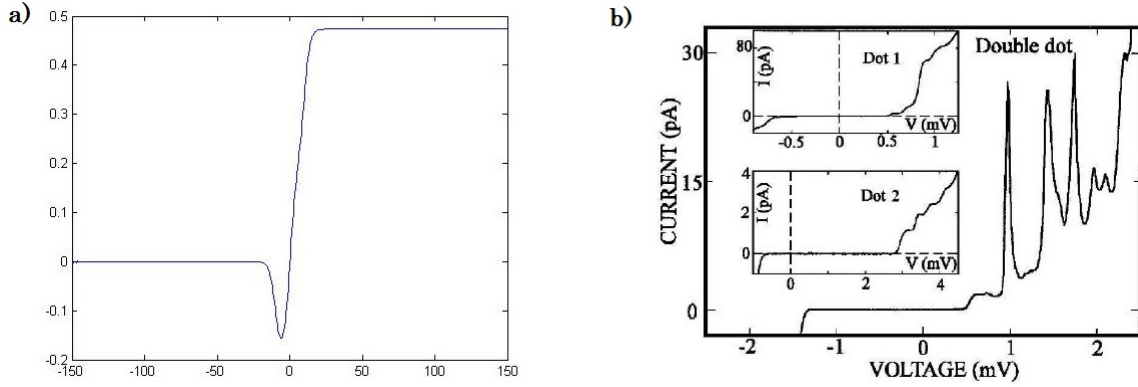


Figure 4.4: (a) I-V curve of the double dot, no current is observed in the negative voltage as a result of Pauli blockade effect, (b) I-V curve of the double dot, showing sharp resonances in the current when two discrete levels align. Upper inset: I-V curve of dot 1. Lower inset: I-V curve of dot 2. Both insets show a suppression of the current at low voltages due to the Coulomb blockade and a stepwise increase of the current due to the discrete energy spectrum of the dot.

The last plot is the one of $I = f(\epsilon_1, \epsilon_2)$, although we won't analyse this graph further in the present thesis, because we cannot compare it with the experimental data, we would need the $dI/d\epsilon_1 = f(\epsilon_1, \epsilon_2)$ diagram, in order to make a comparison with the charge stability diagram.

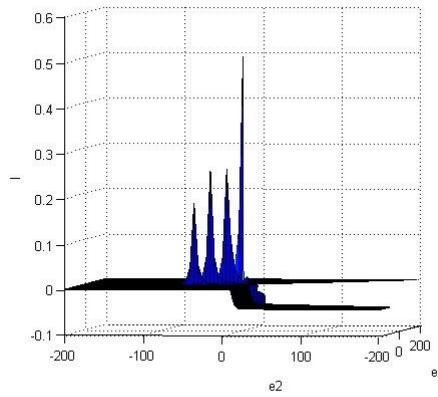


Figure 4.5: Current as a function of the two dots' energies ($I=f(\epsilon_1, \epsilon_2)$) of the double double dot.

Chapter 5

Conclusions

We explained the main features of single and double quantum dots. We found the Hamiltonians describing each system and calculated the elements governing the electron transitions in the system. Using these elements, we created two simulation programs (they are available in the appendices), one for the double dot, with spinless electrons and one for the double dot with electrons with spin. Although we could not include in the present thesis, the $dI/dV_1 = f(\varepsilon_1, \varepsilon_2)$ diagram, which is the charge stability diagram, we could see its qualitative characteristics being in agreement with the experimental results from the $I = f(\varepsilon_1, \varepsilon_2)$ graph. Furthermore we were able to identify the Coulomb blockade in the $I=f(V)$ diagram of both systems and the Pauli blockade in the second program, where we take spin under consideration.

Chapter 6

Appendices

6.1 Double dot without spin (Matlab program)

```
e1=1:1:20;
e2=1:1:20;
t=1;
U=0;
GL=1;
GR=1;
E0=0;
V=10;
mR=V/2;
mL=-V/2;
I=zeros(size(e1,2));
for i=1:1:size(e1,2)
clear A P
for j=1:1:size(e2,2)
Ea = (e1(i) + e2(j))/2 + sqrt((e1(i) - e2(j))^2 + 4 * t^2)/2;
Eb = (e1(i) + e2(j))/2 - sqrt((e1(i) - e2(j))^2 + 4 * t^2)/2;
E2 = Ea + Eb + U;
n = 1 + (e1(i) - Ea)^2;
u = 1/(sqrt(n) * t);
v = (e1(i) - Ea)/(t * sqrt(n));
Ga0 = GL * u^2 * nF(Ea - E0 - mL) + GR * v^2 * nF(Ea - E0 - mR);
Gb0 = GL * v^2 * nF(Eb - E0 - mL) + GR * u^2 * nF(Eb - E0 - mR);
G2a = GL * ((u^2 - v^2) * v)^2 * nF(E2 - Ea - mL) + GR * ((u^2 - v^2) * u)^2 * nF(E2 - Ea - mR);
G2b = GL * ((u^2 - v^2) * u)^2 * nF(E2 - Eb - mL) + GR * ((v^2 - u^2) * v)^2 * nF(E2 - Eb - mR);
G0a = GL * u^2 * (1 - nF(Ea - E0 - mL)) + GR * v^2 * (1 - nF(Ea - E0 - mR));
G0b = GL * v^2 * (1 - nF(Eb - E0 - mL)) + GR * u^2 * (1 - nF(Eb - E0 - mR));
Ga2 = GL * ((u^2 - v^2) * v)^2 * (1 - nF(E2 - Ea - mL)) + GR * ((u^2 - v^2) * u)^2 * (1 - nF(E2 - Ea - mR));
Gb2 = GL * ((u^2 - v^2) * u)^2 * (1 - nF(E2 - Eb - mL)) + GR * ((u^2 - v^2) * v)^2 * (1 - nF(E2 - Eb - mR));
A(1,1) = Ga0;
A(1,2) = -(G0a + G2a);
A(1,3) = 0;
A(1,4) = Ga2;
A(2,1) = Gb0;
A(2,2) = 0;
A(2,3) = -(G0b + G2b);
A(2,4) = Gb2;
A(3,1) = -(Ga0 + Gb0);
A(3,2) = G0a;
```

```

A(3,3) = G0b;
A(3,4) = 0;
A(4,1) = 1;
A(4,2) = 1;
A(4,3) = 1;
A(4,4) = 1;
C(4) = 1;
P=inv(A)*(C');
I(i,j) = P(1) * GL * u^2 * nF(Ea - E0 - mL) - P(2) * GL * u^2 * (1 - nF(Ea - E0 - mL)) + P(1) *
GL * v^2 * nF(Eb - E0 - mL) - P(3) * GL * v^2 * (1 - nF(Eb - E0 - mL)) + P(2) * GL * ((u^2 - v^2) *
v)^2 * nF(E2 - Ea - mL) - P(4) * GL * ((u^2 - v^2) * v)^2 * (1 - nF(E2 - Ea - mL)) + P(3) * GL * ((u^2 -
v^2) * u)^2 * nF(E2 - Eb - mL) - P(4) * GL * ((u^2 - v^2) * u)^2 * (1 - nF(E2 - Eb - mL));
end
end
surf(e2,e1,-I)

```

6.2 Double dot with spin (Matlab program)

```

e1u=e1d=(-200:5:200);
e2u=e2d=(-200:5:200);
t=1;
U12=1;
U22=1;
GL=1;
GR=1;
E0=0;
V=30;
mR=V/2;
mL=-V/2;
I = zeros(size(e1u, 2));
for i=1:1:size(e1u,2)
clear A P
for j=1:1:size(e2u,2)
H2e(1,1) = (e1u(i) + e1u(i) + e2u(j) + e2u(j))/2 + U12;
H2e(2,2) = e1u(i) + e2u(j) + U12;
H2e(3,3) = e1u(i) + e2u(j) + U12;
H2e(4,4) = (e1u(i) + e1u(i) + e2u(j) + e2u(j))/2 + U12;
H2e(5,5) = e2u(j) + e2u(j) + U22;
H2e(4,5) = t/sqrt(2);
H2e(5,4) = t/sqrt(2);
[S, E2] = eig(H2e); u=S(4,1); v=-S(5,1);
GT02u = GL * (1/2) * (nF(E2(4,4) - e2u(j) - mL));
GTp2u = GL * (nF(E2(2,2) - e2u(j) - mL));
GTm2u = 0;
GS12u = GL * (u^2)/2 * (nF(E2(1,1) - e2u(j) - mL)) + GR * (v^2) * (nF(E2(1,1) - e2u(j) - mR));
GS22u = GL * (v^2)/2 * (nF(E2(5,5) - e2u(j) - mL)) + GR * (u^2) * (nF(E2(5,5) - e2u(j) - mR));
GT02d = GL * (1/2) * (nF(E2(4,4) - e2u(j) - mL));
GTp2d = 0;
GTm2d = GL * (nF(E2(3,3) - e2u(j) - mL));
GS12d = GL * (u^2)/2 * (nF(E2(1,1) - e2u(j) - mL)) + GR * (v^2) * (nF(E2(1,1) - e2u(j) - mR));
GS22d = GL * (v^2)/2 * (nF(E2(5,5) - e2u(j) - mL)) + GR * (u^2) * (nF(E2(5,5) - e2u(j) - mR));
G2uT0 = GL * (1/2) * (1 - nF(E2(4,4) - e2u(j) - mL));
G2uTp = GL * (1 - nF(E2(2,2) - e2u(j) - mL));

```

$$\begin{aligned}
G2uTm &= 0; \\
G2uS1 &= GL*(u^2)/2*(1-nF(E2(1,1)-e2u(j)-mL))+GR*(v^2)*(1-nF(E2(1,1)-e2u(j)-mR)); \\
G2uS2 &= GL*(v^2)/2*(1-nF(E2(5,5)-e2u(j)-mL))+GR*(u^2)*(1-nF(E2(5,5)-e2u(j)-mR)); \\
G2dT0 &= GL*(1/2)*(1-nF(E2(4,4)-e2u(j)-mL)); \\
G2dTp &= 0; \\
G2dTm &= GL*(1-nF(E2(3,3)-e2u(j)-mL)); \\
G2dS1 &= GL*(u^2)/2*(1-nF(E2(1,1)-e2u(j)-mL))+GR*(v^2)*(1-nF(E2(1,1)-e2u(j)-mR)); \\
G2dS2 &= GL*(v^2)/2*(1-nF(E2(5,5)-e2u(j)-mL))+GR*(u^2)*(1-nF(E2(5,5)-e2u(j)-mR)); \\
GT01u &= GR*(1/2)*(1-nF(E2(4,4)-(e1u(i)+e2u(j)+e2u(j)+U12+U22)-mR)); GTp1u = \\
&GR*(1-nF(E2(2,2)-(e1u(i)+e2u(j)+e2u(j)+U12+U22)-mR)); \\
GTm1u &= 0; \\
GS11u &= GL*(v^2)*(1-nF(E2(1,1)-(e1u(i)+e2u(j)+e2u(j)+U12+U22)-mL))+GR*(u^2)/2* \\
&(1-nF(E2(1,1)-(e1u(i)+e2u(j)+e2u(j)+U12+U22)-mR)); \\
GS21u &= GL*(u^2)*(1-nF(E2(5,5)-(e1u(i)+e2u(j)+e2u(j)+U12+U22)-mL))+GR*(v^2)/2* \\
&(1-nF(E2(5,5)-(e1u(i)+e2u(j)+e2u(j)+U12+U22)-mR)); \\
GT01d &= GR*(1/2)*(1-nF(E2(4,4)-(e1u(i)+e2u(j)+e2u(j)+U12+U22)-mR)); \\
GTp1d &= 0; \\
GTm1d &= GR*(1-nF(E2(3,3)-(e1u(i)+e2u(j)+e2u(j)+U12+U22)-mR)); \\
GS11d &= GL*(v^2)*(1-nF(E2(1,1)-(e1u(i)+e2u(j)+e2u(j)+U12+U22)-mL))+GR*(u^2)/2* \\
&(1-nF(E2(1,1)-(e1u(i)+e2u(j)+e2u(j)+U12+U22)-mR)); \\
GS21d &= GL*(u^2)*(1-nF(E2(5,5)-(e1u(i)+e2u(j)+e2u(j)+U12+U22)-mL))+GR*(v^2)/2* \\
&(1-nF(E2(5,5)-(e1u(i)+e2u(j)+e2u(j)+U12+U22)-mR)); \\
G1uT0 &= GR*(1/2)*nF(E2(4,4)-(e1u(i)+e2u(j)+e2u(j)+U12+U22)-mR); \\
G1uTp &= GR*nF(E2(2,2)-(e1u(i)+e2u(j)+e2u(j)+U12+U22)-mR); \\
G1uTm &= 0; \\
G1uS1 &= GL*(v^2)*nF(E2(1,1)-(e1u(i)+e2u(j)+e2u(j)+U12+U22)-mL)+GR*(u^2)/2* \\
&nF(E2(1,1)-(e1u(i)+e2u(j)+e2u(j)+U12+U22)-mR); \\
G1uS2 &= GL*(u^2)*nF(E2(5,5)-(e1u(i)+e2u(j)+e2u(j)+U12+U22)-mL)+GR*(v^2)/2* \\
&nF(E2(5,5)-(e1u(i)+e2u(j)+e2u(j)+U12+U22)-mR); \\
G1dT0 &= GL*(1/2)*nF(E2(4,4)-(e1u(i)+e2u(j)+e2u(j)+U12+U22)-mL); \\
G1dTp &= 0; \\
G1dTm &= GR*nF(E2(3,3)-(e1u(i)+e2u(j)+e2u(j)+U12+U22)-mR); \\
G1dS1 &= GL*(v^2)*nF(E2(1,1)-(e1u(i)+e2u(j)+e2u(j)+U12+U22)-mL)+GR*(u^2)/2* \\
&nF(E2(1,1)-(e1u(i)+e2u(j)+e2u(j)+U12+U22)-mR); \\
G1dS2 &= GL*(u^2)*nF(E2(5,5)-(e1u(i)+e2u(j)+e2u(j)+U12+U22)-mL)+GR*(v^2)/2* \\
&nF(E2(5,5)-(e1u(i)+e2u(j)+e2u(j)+U12+U22)-mR); \\
A(1,1) &= -(GT01u+GTp1u+GTm1u+GS11u+GS21u); \\
A(1,5) &= G1uT0; \\
A(1,6) &= G1uTp; \\
A(1,7) &= G1uTm; \\
A(1,8) &= G1uS1; \\
A(1,9) &= G1uS2; \\
A(2,2) &= -(GT01d+GTp1d+GTm1d+GS11d+GS21d); \\
A(2,5) &= G1dT0; \\
A(2,6) &= G1dTp; \\
A(2,7) &= G1dTm; \\
A(2,8) &= G1dS1; \\
A(2,9) &= G1dS2; \\
A(3,3) &= -(GT02u+GTp2u+GTm2u+GS12u+GS22u); \\
A(3,5) &= G2uT0; \\
A(3,6) &= G2uTp; \\
A(3,7) &= G2uTm; \\
A(3,8) &= G2uS1;
\end{aligned}$$

```

A(3, 9) = G2uS2;
A(4, 4) = -(GT02d + GTP2d + GTm2d + GS12d + GS22d);
A(4, 5) = G2dT0;
A(4, 6) = G2dTp;
A(4, 7) = G2dTm;
A(4, 8) = G2dS1;
A(4, 9) = G2dS2;
A(5, 1) = GT01u;
(5, 2) = GT01d;
A(5, 3) = GT02u;
A(5, 4) = GT02d;
A(5, 5) = -(G1uT0 + G1dT0 + G2uT0 + G2dT0);
A(6, 1) = GTP1u;
A(6, 2) = GTP1d;
A(6, 3) = GTP2u;
A(6, 4) = GTP2d;
A(6, 6) = -(G1uTp + G1dTp + G2uTp + G2dTp);
A(7, 1) = GTm1u;
A(7, 2) = GTm1d;
A(7, 3) = GTm2u;
A(7, 4) = GTm2d;
A(7, 7) = -(G1uTm + G1dTm + G2uTm + G2dTm);
A(8, 1) = GS11u;
A(8, 2) = GS11d;
A(8, 3) = GS12u;
A(8, 4) = GS12d;
A(8, 8) = -(G1uS1 + G1dS1 + G2uS1 + G2dS1);
A(9, 1 : 9) = 1;
C(9)=1;
P = inv(A) * (C');
I(i, j) = P(5) * (GL * (1/2) * nF(E2(4, 4) - (e1u(i) + e2u(j) + e2u(j) + U12 + U22) - mL) - GL * (1/2) *
(1 - nF(E2(4, 4) - e2u(j) - mL)) - GL * (1/2) * (1 - nF(E2(4, 4) - e2u(j) - mL))) + P(6) * (-GL *
(1 - nF(E2(2, 2) - e2u(j) - mL))) + P(7) * (-GL * (1 - nF(E2(3, 3) - e2u(j) - mL))) + P(8) * (GL *
(v^2) * nF(E2(1, 1) - (e1u(i) + e2u(j) + e2u(j) + U12 + U22) - mL) + GL * (v^2) * nF(E2(1, 1) - (e1u(i) +
e2u(j) + e2u(j) + U12 + U22) - mL) - GL * (u^2)/2 * (1 - nF(E2(1, 1) - e2u(j) - mL)) - GL * (u^2)/2 *
(1 - nF(E2(1, 1) - e2u(j) - mL))) + P(9) * (GL * (u^2) * nF(E2(5, 5) - (e1u(i) + e2u(j) + e2u(j) +
U12 + U22) - mL) + GL * (u^2) * nF(E2(5, 5) - (e1u(i) + e2u(j) + e2u(j) + U12 + U22) - mL) - GL *
(v^2)/2 * (1 - nF(E2(5, 5) - e2u(j) - mL)) - GL * (v^2)/2 * (1 - nF(E2(5, 5) - e2u(j) - mL))) + P(1) *
(-GL * (v^2) * (1 - nF(E2(1, 1) - (e1u(i) + e2u(j) + e2u(j) + U12 + U22) - mL)) - GL * (u^2) * (1 -
nF(E2(5, 5) - (e1u(i) + e2u(j) + e2u(j) + U12 + U22) - mL))) + P(2) * (-GL * (v^2) * (1 - nF(E2(1, 1) -
(e1u(i) + e2u(j) + e2u(j) + U12 + U22) - mL)) - GL * (u^2) * (1 - nF(E2(5, 5) - (e1u(i) + e2u(j) +
e2u(j) + U12 + U22) - mL))) + P(3) * (GL * (1/2) * (nF(E2(4, 4) - e2u(j) - mL)) + GL * (nF(E2(2, 2) -
e2u(j) - mL)) + GL * (u^2)/2 * (nF(E2(1, 1) - e2u(j) - mL)) + GL * (v^2)/2 * (nF(E2(5, 5) - e2u(j) -
mL))) + P(4) * (GL * (1/2) * (nF(E2(4, 4) - e2u(j) - mL)) + GL * (nF(E2(3, 3) - e2u(j) - mL)) +
GL * (u^2)/2 * (nF(E2(1, 1) - e2u(j) - mL)) + GL * (v^2)/2 * (nF(E2(5, 5) - e2u(j) - mL)));
end
end
contourf(e1u,e2u,-I)

```

Bibliography

- [1] Henrik Bruus, Karsten Flensberg *Many-Body Quantum Theory in Condensed Matter Physics* 2004: Oxford University Press.
- [2] Thomas Ihn *Semiconductor Nanostructures: Quantum states and electronic transport* 2010: Oxford University Press.
- [3] R. Hanson, L. P. Kouwenhoven, J. R. Petta, S. Tarucha, and L. M. K. Vandersypen *Spins in few-electron quantum dots [Rev. Mod. Phys. 79]* 2007: The American Physical Society.
- [4] W. G. van der Wiel, S. De Franceschi, J. M. Elzerman, T. Fujisawa, S. Tarucha, L. P. Kouwenhoven *Electron transport through double quantum dots [Rev. Mod. Phys. 75]* 2002: The American Physical Society.
- [5] N. Mason, M. J. Biercuk, C. M. Marcus *Local Gate Control of a Carbon Nanotube Double Quantum Dot* 2004: Science.